XXXII
International School of Hydraulics
28 - 31 May · 2012 · Łochów · Poland

# Hydrodynamics of Undular Free Surface Flows

**Subhasish Dey, Sujit K. Bose**
Indian Institute of Technology, Kharagpur, India
**and**
**Oscar Castro-Orgaz**
Instituto de Agricultura Sostenible, CSIC, Cordoba, Spain

# Introduction

Free surface profiles of open channel flows exhibit considerable undulations, depending on the flow and the boundary conditions

- An undular hydraulic jump can occur, when the approach flow Froude number slightly exceeds unity

Undulations of the channel boundary that can induce undular free surface profiles are:

- Flow over submerged obstacles
- Flow over wavy boundaries

# Objective of the Present Study

To provide a theoretical analysis for the following types of steady undular free surface flows:

- Undular hydraulic jump on a plane smooth boundary
- Flow over a submerged hemi-cylindrical boss
- Flow over a sinusoidal boundary of a channel

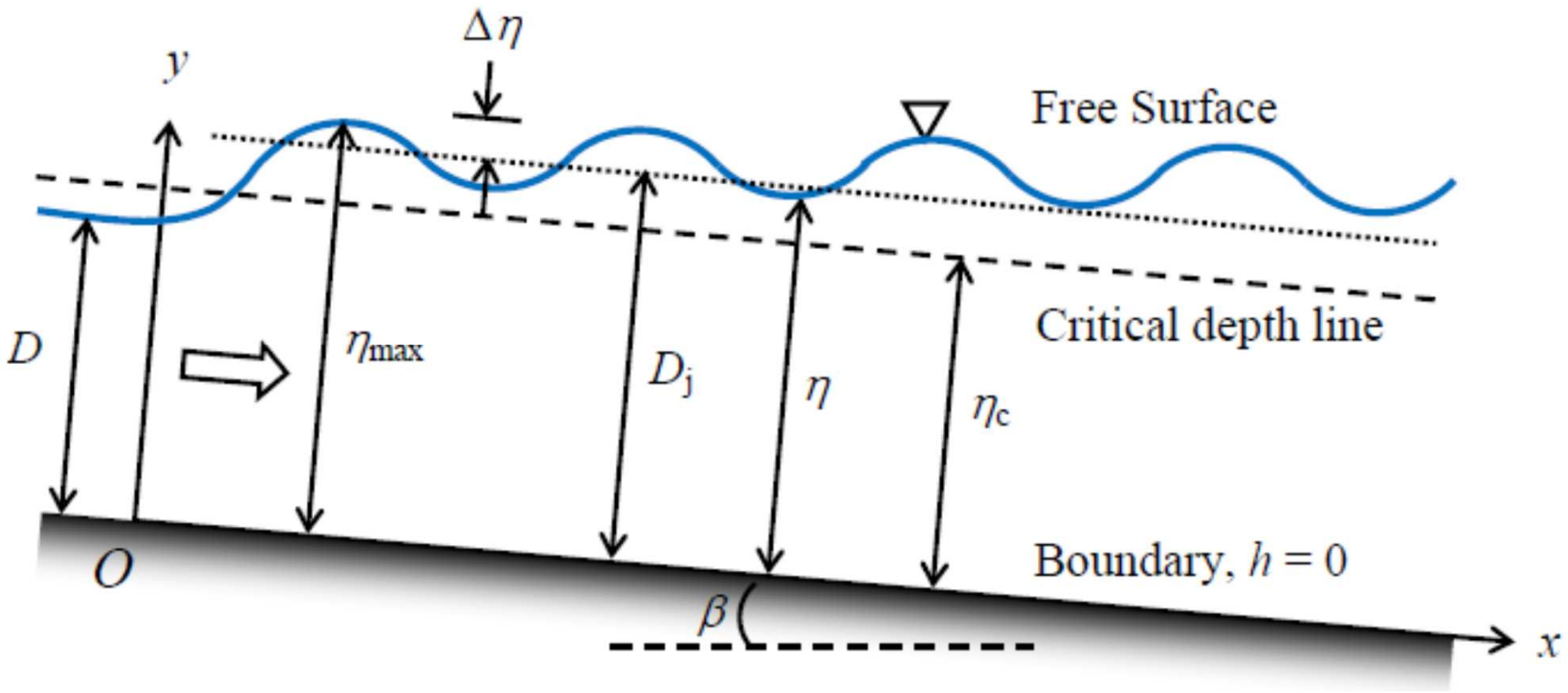


Sketch of an undular hydraulic jump

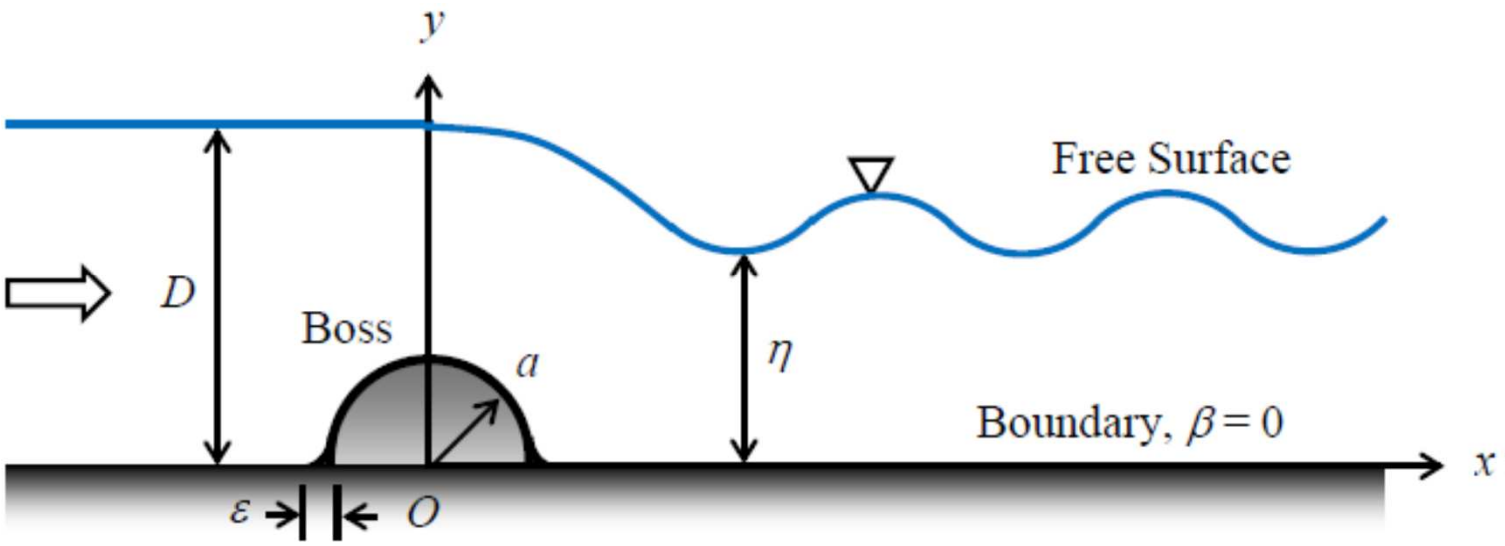


Sketch of flow over a hemi-cylindrical boss

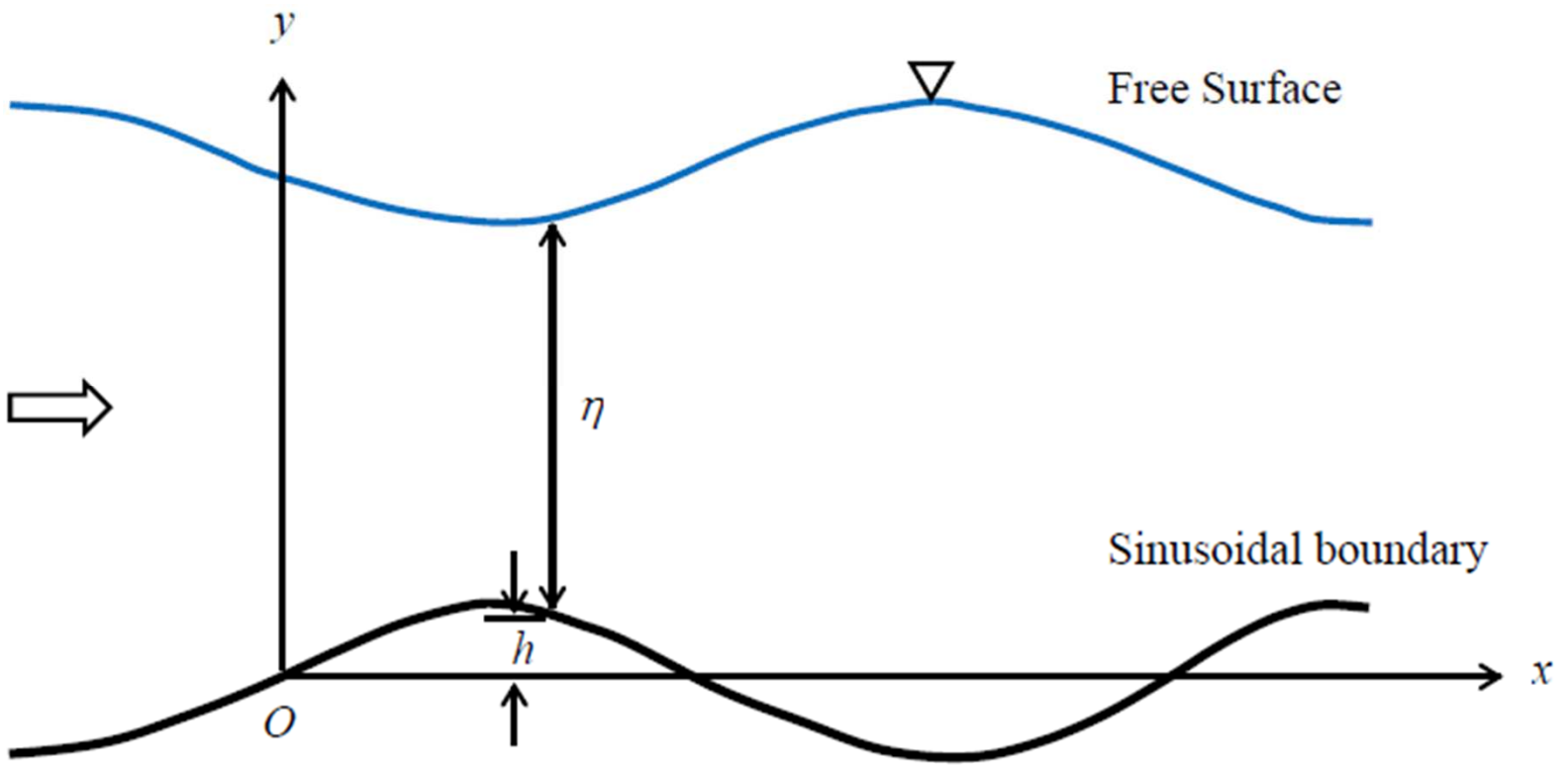


Sketch of flow over a sinusoidal boundary of a channel

# Previous Studies

## *Undular Hydraulic Jump Analyzed by Potential Flow Theory*

Fawer (1937): The first to treat as a series of cnoidal waves that existed following the first wave crest, but a transition from supercritical to subcritical flow was not considered

Benjamin and Lighthill (1954) and Mandrup-Andersen (1978): Hypothesized the first wave crest portion by a solitary wave and the downstream flow portion by a series of subcritical cnoidal waves

Iwasa (1955): Analyzed undular hydraulic jumps as a connection of solitary and cnoidal waves at the location of critical point $F_0 = 1$

Fawer (1937) and Mandrup-Andersen (1978): Preferred a subcritical point ahead of the first wave crest

## *Undular Hydraulic Jump Analyzed by Potential Flow Theory*

- It is a traditional theoretical approach to have continuity at the meeting point of the solitary and the cnoidal wave portions to define the entire undular hydraulic jump profile

- In this way, it takes into account the transitional flow from supercritical to subcritical flow induced by the boundary resistance

## *Undular Hydraulic Jump Analyzed by Viscous Flow Theory*

Kaufmann (1934): Found an exponentially decaying harmonic function for the free surface profiles

Mandrup-Anderson (1978) and Montes and Chanson (1998): Provided improved theory by using Boussinesq-type energy equation

Montes (1998): Applied perturbation analysis to treat the turbulent flow equations. He found that the streamwise velocity obeys the 1/7th power law of the wall

Hager and Hutter (1984): Used an improved Boussinesq-type energy equation obtained from the Euler equations. They accounted for the energy dissipation by merging upstream and downstream solutions at a suitably chosen position on the undular hydraulic jump profiles

## *Undular Hydraulic Jump Analyzed by Viscous Flow Theory*

Grillhofer and Schneider (2003): Gave an asymptotic analysis of the turbulent flow equations. They solved a third order ordinary-differential equation for the free surface profiles leading to an undular hydraulic jump

Castro-Orgaz (2010): Put forward a simplified method to figure out the oscillatory boundary layer characteristics in a weakly undular hydraulic jump

A number of good experimental studies done by Chanson (1993, 1995, 2000); Chanson and Montes (1995); Reinauer and Hager (1995); Ohtsu et al. (2001, 2003) and Gotoh et al. (2005)

## *Flows over Isolated-Submerged Obstacles*

Good and Joubert (1968), Sforza and Mons (1970), Dimaczek et al. (1989), Schulte and Rouvé (1986), Durão et al. (1991), Akoz and Kirkgoz (2009) and Akoz et al. (2010):

Studied flow over a circular or rectangular cylinder placed on the channel bottom in the context of the wake flow behind the two-dimensional obstacles

## *Flows over Undular Channel Boundaries*

Zhaoshun and Zhan (1989), Patel et al. (1991), Nakayama and Sakio (2002) and Tsai and Chou (2008): Used numerical techniques to solve the problems of undular channel boundaries

Henderson (1964): Used the standard backwater approach

Iwasa and Kennedy (1968): Used Boussinesq-type energy equations in a boundary-fitted system of reference, thereby accounting for the channel boundary curvature in the governing equations

Motzfeld (1937) and Hsu and Kennedy (1971): Observed a phase lag in the boundary pressure distribution relative to the sinusoidal boundary

Mizumura (1995): Gave the detailed difference of the free surface profiles in the supercritical and subcritical flows over rigid wavy boundaries by using the potential flow theory

# Governing Equations of Undular Free Surface Flows

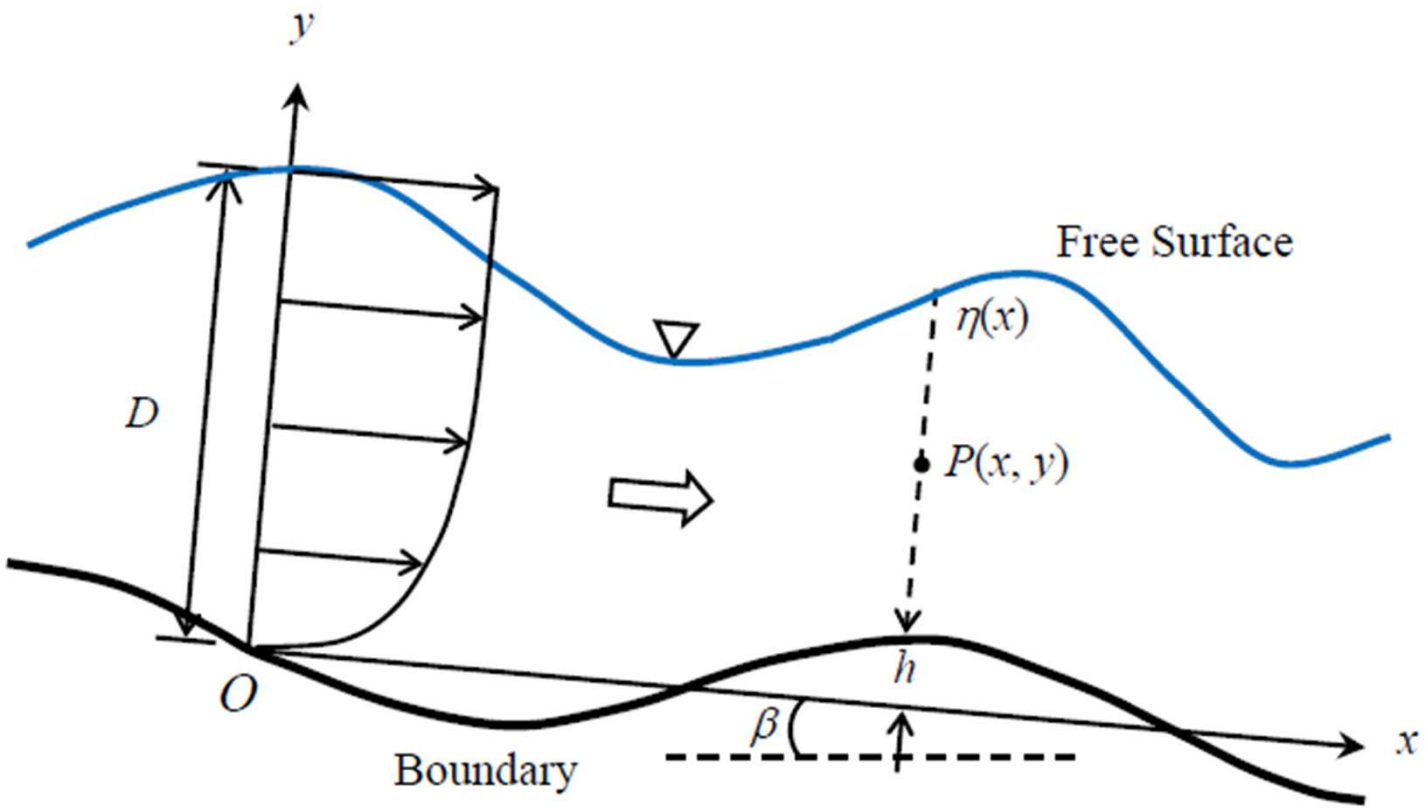


**Fig. 1** Definition sketch of curvilinear flow over an undular boundary

The Continuity equation

$$\frac{\partial}{\partial t}(\eta - h) + \frac{\partial}{\partial x}[(\eta - h)U] = 0 \qquad (1)$$

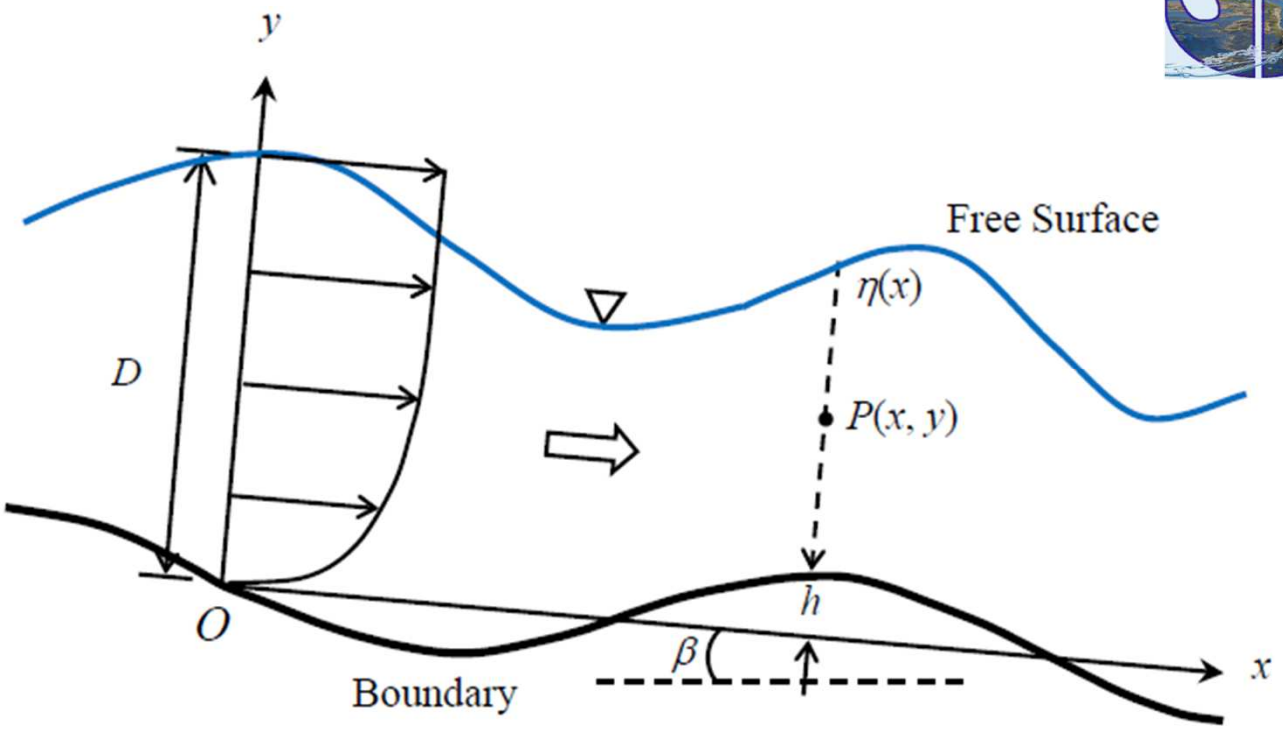


Bed inclined at an angle $\beta$ with the horizontal

$t$ = time

$U(x, t)$ = depth-averaged streamwise velocity at $P(x, y) = (\eta - h)^{-1} \int_h^{\eta} \bar{u}(x, y, t)dy$

$h(x)$ = elevation of the boundary profile from the mean bed level

$\bar{u}$ = time-averaged streamwise velocity at point $P(x, y)$

$\eta(x, t)$ = free surface elevation from the mean level

The momentum equation for curvilinear boundaries as obtained by Bose and Dey (2007, 2009):

$$\frac{\partial U}{\partial t}+U\frac{\partial U}{\partial x}+\frac{2}{5(\eta-h)}\cdot\frac{\partial}{\partial x}\left[(\eta-h)^2U^2\left(\frac{\partial^2\eta}{\partial x^2}+\frac{7}{16}\cdot\frac{\partial^2 h}{\partial x^2}\right)\right]-\frac{7}{22}(\eta-h)^2\frac{\partial^3 U}{\partial t\partial x^2}$$
$$+g\cos\beta\frac{\partial\eta}{\partial x}-g\sin\beta+\frac{\tau_0}{\rho(\eta-h)}=0 \qquad (2)$$

According to the Manning equation, the $\tau_0$ is given by $\rho g n^2 U^2/(\eta-h)^{1/3}$ where $n$ is the Manning roughness coefficient

The continuity equation, Eq. (1), thus

$$(\eta-h)U=q \qquad (3)$$

$q$ = discharge per unit width across the section of interest

Using continuity equation, i.e. Eq. (3), the momentum equation, i.e. Eq. (2), becomes

$$\frac{d^3\eta}{dx^3}+\frac{5}{2}\left[\frac{g(\eta-h)\cos\beta}{q^2}-\frac{1}{(\eta-h)^2}\right]\frac{d\eta}{dx}+\frac{7}{16}\cdot\frac{d^3h}{dx^3}+\frac{5}{2(\eta-h)^2}\cdot\frac{dh}{dx}$$
$$+\frac{5}{2q^2}\left[\frac{\tau_0}{\rho}-g(\eta-h)\sin\beta\right]=0 \qquad (4)$$

Eq. (4) determines the steady-state free surface profiles,
when undular boundary profile $h(x)$, bed inclination $\beta$ and discharge $q$ are known parameters

# Undular Hydraulic Jump over a Plane Sloping Boundary

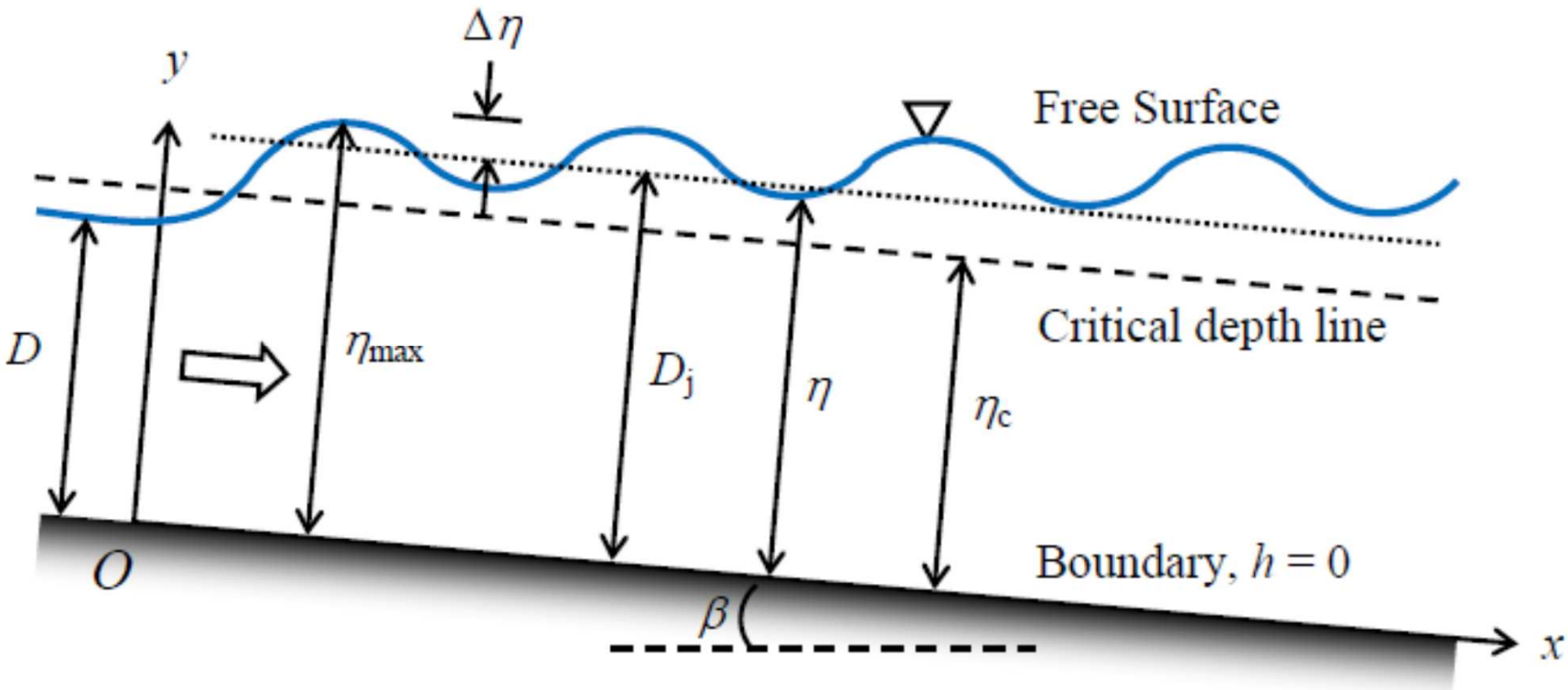


**Fig. 2** Schematic of an undular hydraulic jump on a sloping boundary

Here, $h(x) = 0$. Therefore, Eq. (4) applies as

$$\frac{d^3\eta}{dx^3}+\frac{5}{2}\left(\frac{g\eta\cos\beta}{q^2}-\frac{1}{\eta^2}\right)\frac{d\eta}{dx}+\frac{5}{2q^2}\left(\frac{\tau_0}{\rho}-g\eta\sin\beta\right)=0 \qquad (5)$$

The phenomenon of undular hydraulic jump is treated as an **instability** in the flow governed by Eq. (5)

Let, the flow depth be $D$ at the origin $O$ (Fig. 2). In the surroundings of $O$, Eq. (5) with $\eta = D$ yields

$$\tau_{0D} = \rho g D \sin\beta \qquad (6)$$

where $\tau_{0D}$ is $\rho g n^2 q^2 / D^{7/3}$

For an unstable solution of Eq. (5), let $\eta\,(x >> 0) = D(1 + \eta_1)$. Then, we can write to the first order approximation as

$$\tau_0 = \frac{\rho g n^2 q^2}{D^{7/3}}\left(1 - \frac{7}{3}\eta_1\right) = \rho g D \sin\beta\left(1 - \frac{7}{3}\eta_1\right) \qquad (7)$$

Eq. (5) becomes

$$\frac{d^3\eta_1}{dx^3}+\frac{5}{2}\left(\frac{gD\cos\beta}{q^2}-\frac{1}{D^2}\right)\frac{d\eta_1}{dx}-\frac{25}{3}\cdot\frac{g\sin\beta}{q^2}\eta_1=0 \qquad (8)$$

Introducing flow Froude number $F_0 \Rightarrow q^2 = F_0{}^2 gD^3$, Eq. (8) becomes

$$\frac{d^3\eta_1}{dx^3}+\frac{5}{2D^2}\left(\frac{\cos\beta}{F_0^2}-1\right)\frac{d\eta_1}{dx}-\frac{25}{3}\cdot\frac{\sin\beta}{F_0^2D^3}\eta_1=0 \qquad (9)$$

Eq. (9) is a third-order linear ODE. Its solution is of the form $\eta_1 = E \exp(\lambda x)$, having a constant $E$ and a coefficient $\lambda$. Inserting it into Eq. (9), $\lambda$ must satisfy the cubic equation. Then

$$(D\lambda)^3+\frac{5}{2}\left(\frac{\cos\beta}{F_0^2}-1\right)D\lambda-\frac{25}{3}\cdot\frac{1}{F_0^2}\sin\beta=0 \qquad (10)$$

Since the boundary inclination $\beta$ is usually very small, the three roots of Eq. (10) are approximated as

$$D\lambda \approx \frac{10}{3}\cdot\frac{\sin\beta}{F_0^2-\cos\beta} \quad \text{and} \quad \frac{5}{3}\cdot\frac{\sin\beta}{F_0^2-\cos\beta}\pm\left[\frac{5}{2}\cdot\left(1-\frac{\cos\beta}{F_0^2}\right)\right]^{0.5} \qquad (11)$$

When $F_0^2 < \cos\beta$, the real parts of $D\lambda$ are all negative, referring to the decaying solutions. It indicates that there is no instability in the solution due to an exponential decrease in flow depth

Alternatively, when $F_0^2 > \cos\beta$, all the roots are real and two of them are positive. It suggests an instability in fluid motion, resulting in an undular hydraulic jump, as observed in experiments

More specifically, all three roots of Eq. (10) are real, when $\hat{q}^3 + \hat{r}^2 < 0$

where $\hat{q} = \frac{5}{6} \cdot \left( \frac{\cos\beta}{F_0^2} - 1 \right)$ and $\hat{r} = \frac{25}{6} \cdot \frac{\sin\beta}{F_0^2}$ (12)

The condition for real roots on simplification is as follows:

$$(\cos\beta - F_0^2)^3 + 30 F_0^2 \sin^2\beta < 0 \quad (13)$$

Eq. (13) is satisfied if $F_0^2$ to some extent exceeds $\cos\beta$, as $\sin^2\beta$ is very small

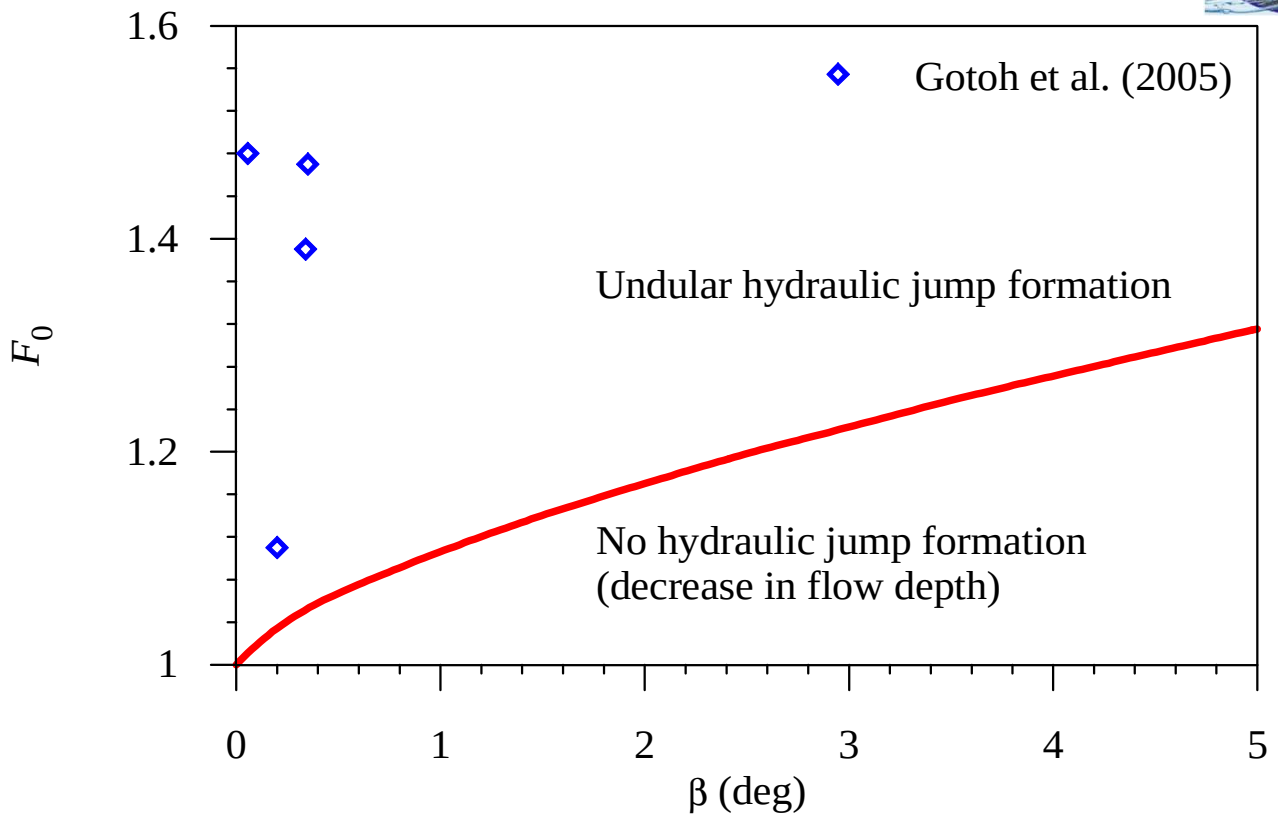


**Fig. 3** $F_0$ versus $\beta$ as threshold condition for the formation of an undular hydraulic jump

The threshold of an undular hydraulic jump corresponds to a monotonic increase of $F_0$ with $\beta$

A negative value of the LHS of Eq. (13) refers to the zone of upper side of the curve, which is the instability zone resulting in an undular hydraulic jump. The experimental data plots lie on this zone of the threshold curve

For plotting free surface profiles, Eq. (5) is expressed in normalized form

$$\frac{d^3\hat{\eta}}{d\hat{x}^3}+\frac{5}{2}\left(\frac{\hat{\eta}}{F_0^2}\cos\beta-\frac{1}{\hat{\eta}^2}\right)\frac{d\hat{\eta}}{d\hat{x}}+\frac{5}{2}\left(\frac{\Omega}{\hat{\eta}^{2/3}}-\frac{\hat{\eta}}{F_0^2}\sin\beta\right)=0 \qquad (14)$$

where $\hat{\eta} = \eta/D$; $\hat{x} = x/D$; and $\Omega = gn^2/D^{1/3}$, termed resistance parameter

Numerical Solution:

The initial conditions are:

At $\hat{x}=0, \hat{\eta}=1, d\hat{\eta}/d\hat{x}=0$ and $d^2\hat{\eta}/d\hat{x}^2=0.01$ (say) a small value

The value of $\Omega$ = 0.004 relevant for a smooth boundary is considered

Eq. (14) is solved for the given values of $F_0$ and $\beta$ by the Runge-Kutta method

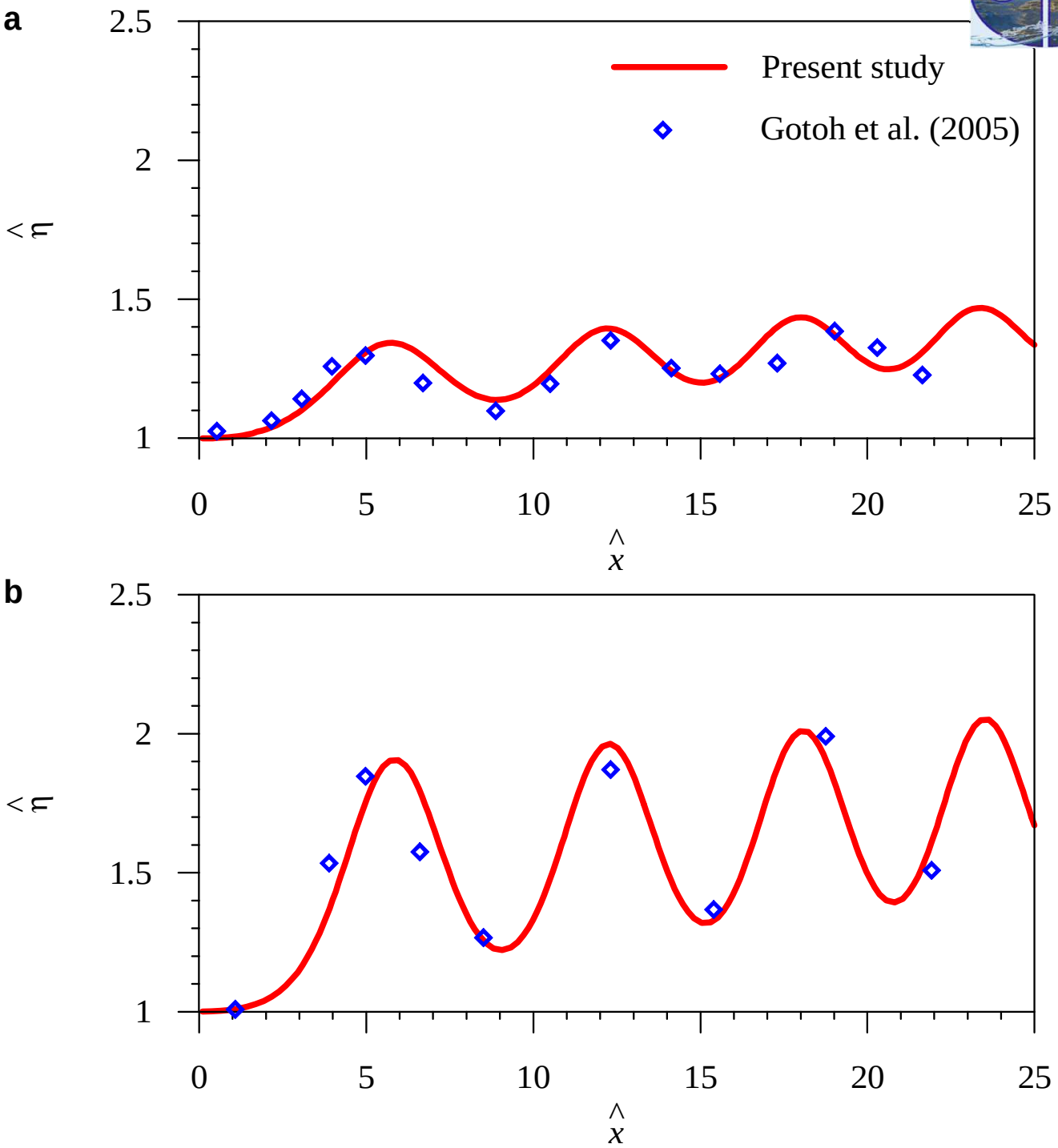


**Fig. 4** Normalized profiles of undular hydraulic jumps for (**a**) $F_0$ = 1.11 and $\tan\beta$ = 0.00355 and (***b***) $F_0$ = 1.39 and $\tan\beta$ = 0.00588

- The computed free surface profiles in general agree well with the experimental data, although a slight discrepancy is apparent in the third wave portion

- The discrepancy may be attributed to the sidewall effect on an experimental flume that could induce lateral instability resulting in shifting of the consecutive crests of the undulations at the free surface

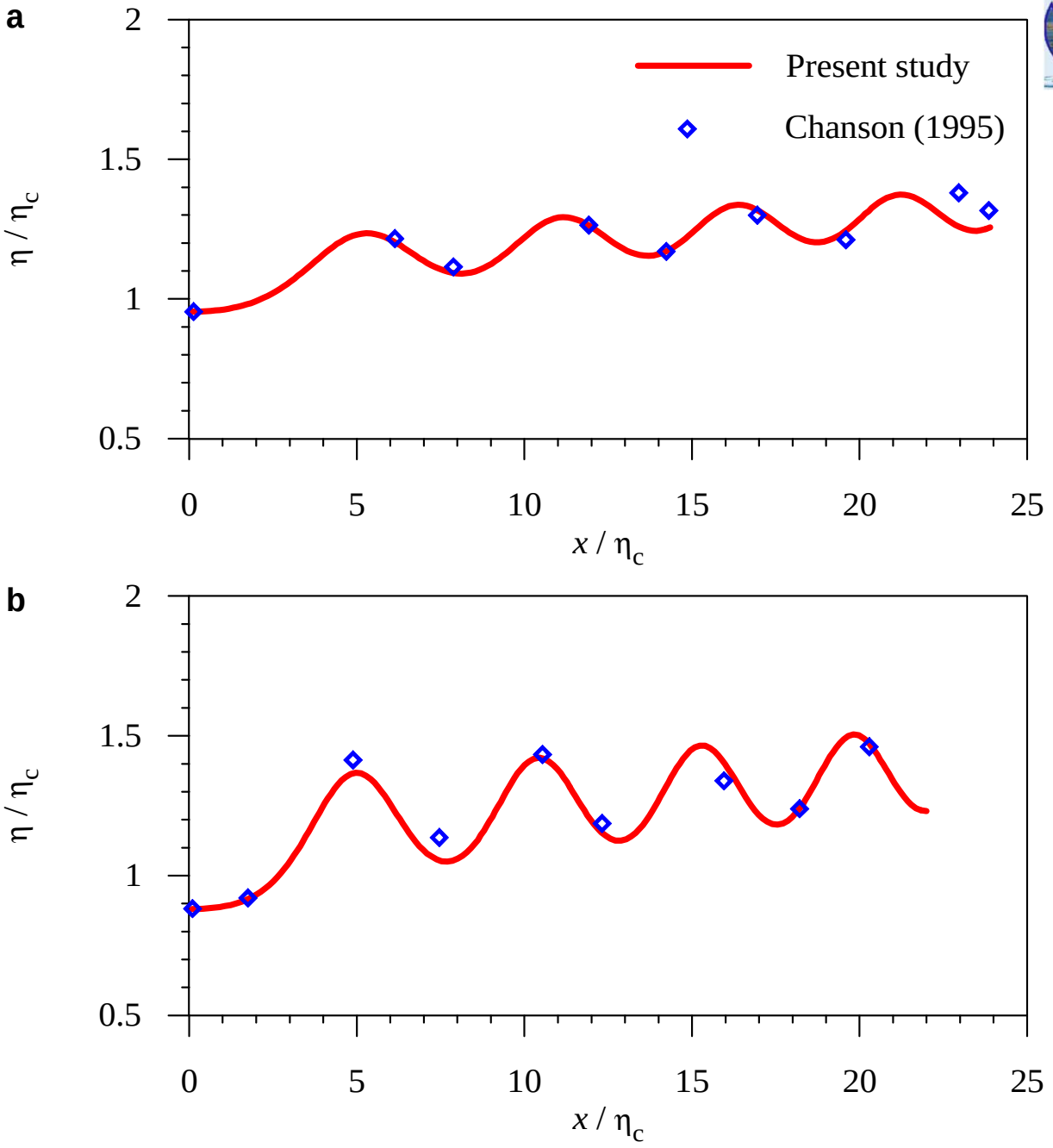


**Fig. 5** Normalized profiles of undular hydraulic jumps for (**a**) $F_0$ = 1.07 and tan$\beta$ = 0.00433 and (**b**) $F_0$ = 1.21 and tan$\beta$ = 0.00567

The experimental data of Chanson (1995) are in agreement with the computed profiles

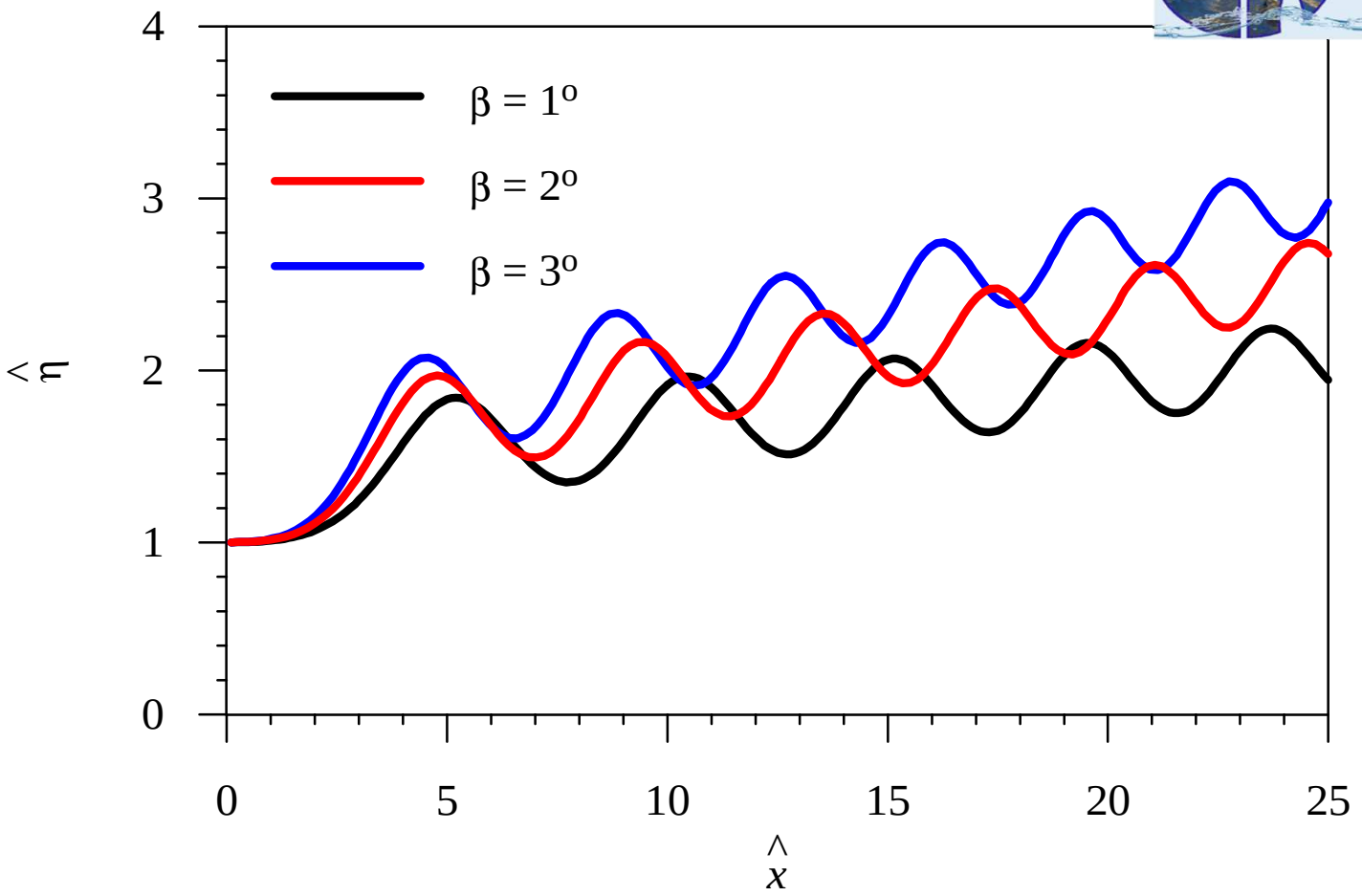


**Fig. 6** Normalized profiles of undular hydraulic jumps for $\beta$ = 1, 2 and 3° and $F_0$ = 1.3

The undular free surface profiles are elevated progressively with an increase in boundary inclination $\beta$

The amplitude of the free surface waves decreases with distance $x$ becoming a flat surface at far downstream

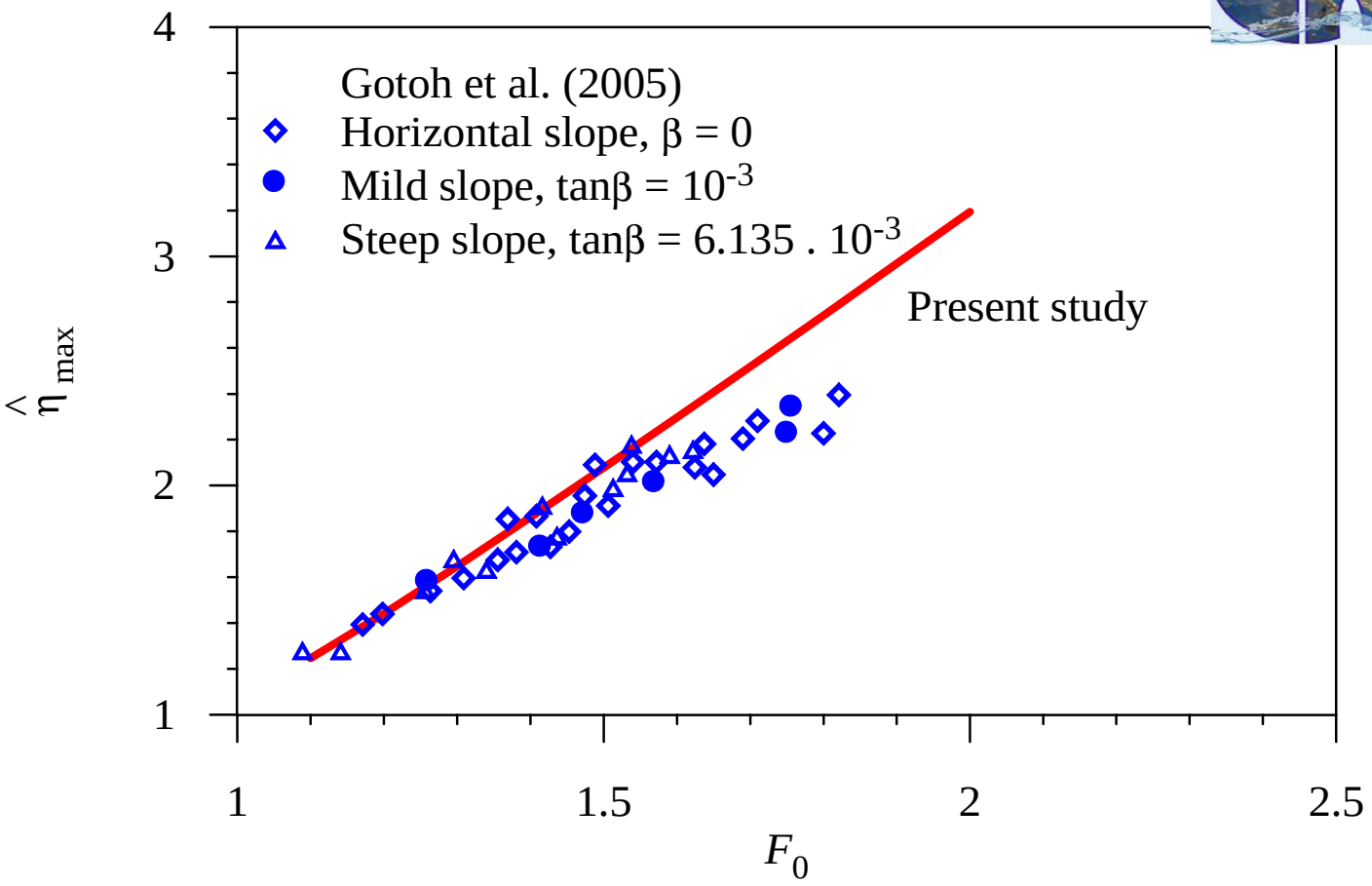


**Fig. 7** Normalized elevation of first wave crest as a function of $F_0$

The $\hat{\eta}_m = \eta_{max}/D$ increases with an increase in $F_0$

The curves are not apparently different for the small variation of $\beta$; such as $\beta = 0°$, arctan(1/1000) and arctan(1/163), which correspond to the horizontal, mild and steep slopes, respectively

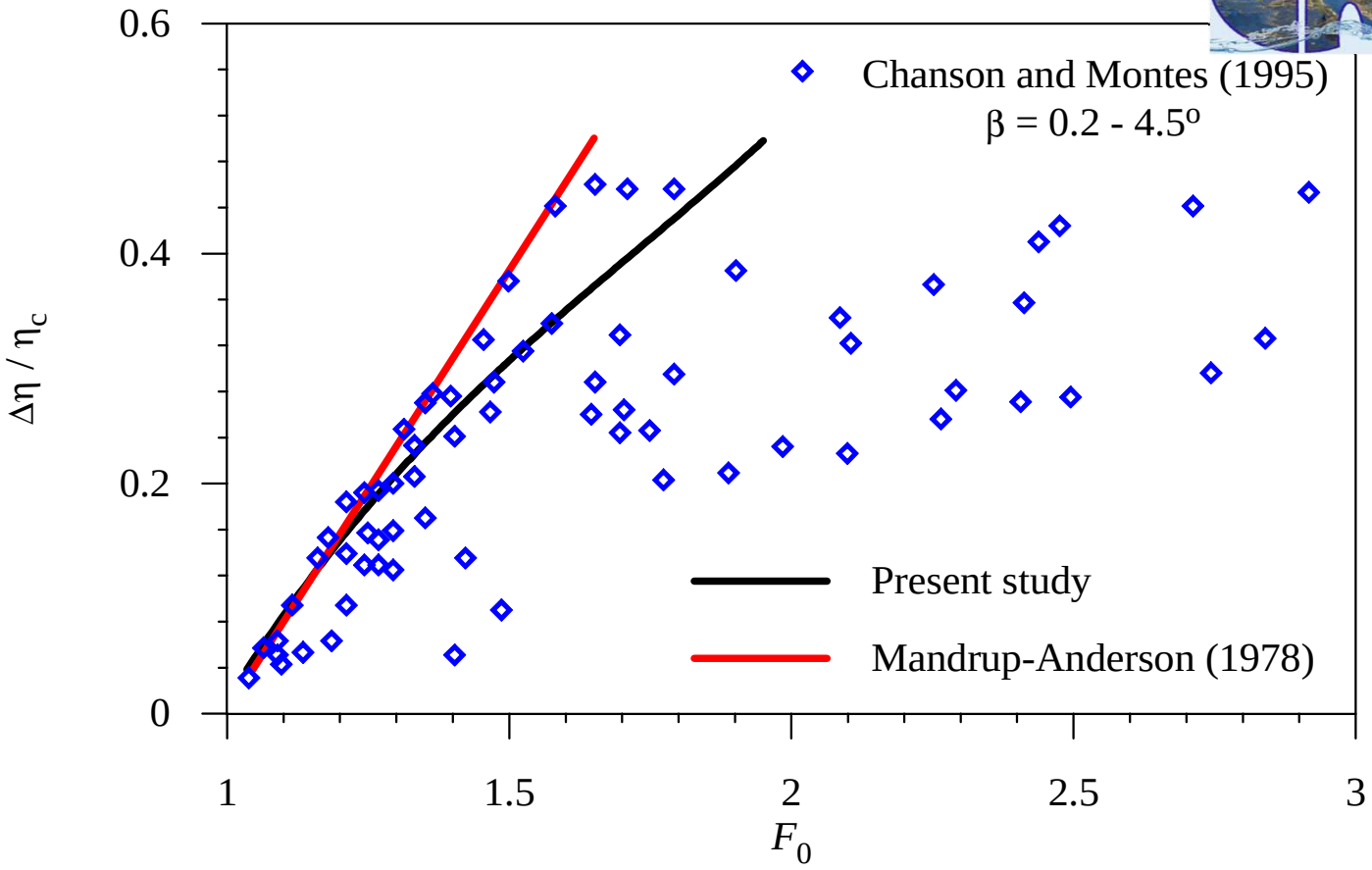


**Fig. 8** Normalized first wave height $\Delta\eta/\eta_c$ as a function of $F_0$

- The $\Delta\eta/\eta_c$ varies monotonically with an increase in $F_0$
- There is some agreement between the computed curve of present study and that obtained from the Boussinesq equation developed by Mandrup-Anderson (1978) for $F_0 < 1.4$
- But a disagreement is always prevalent for the higher values of $F_0$

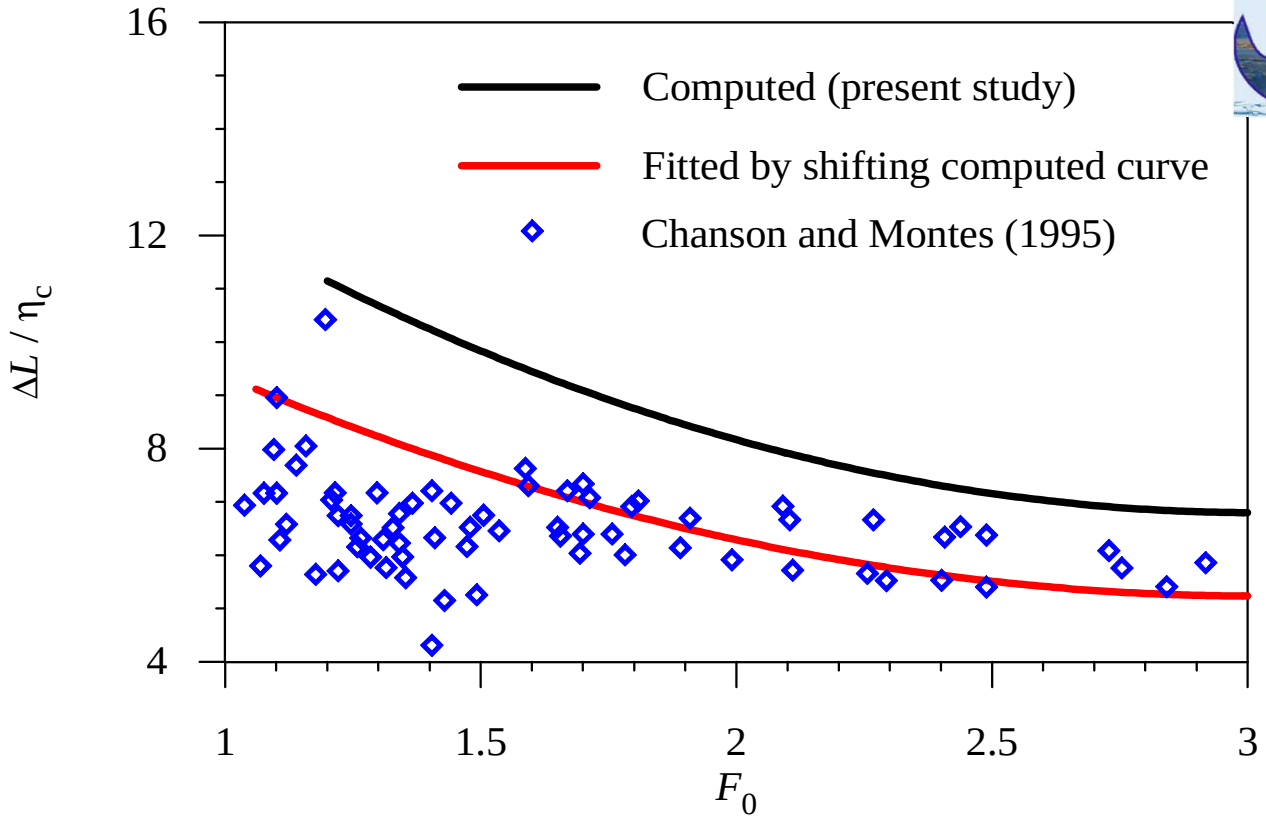


**Fig. 9** Normalized length of first wave $\Delta L/\eta_c$ as a function of $F_0$

- The $\Delta L/\eta_c$ diminishes with $F_0$ becoming independent of $F_0$ for $F_0 > 3$
- Due to the backwater effects a reduction in wave length of undular hydraulic jumps is usually prevalent
- The factor 0.77 shows the degree of discrepancy that exists between the theoretical curve and the experimental data of Chanson and Montes (1995)
- Present theory overestimates the experimental data on first wave length

# Flow over a Hemi-Cylindrical Boss

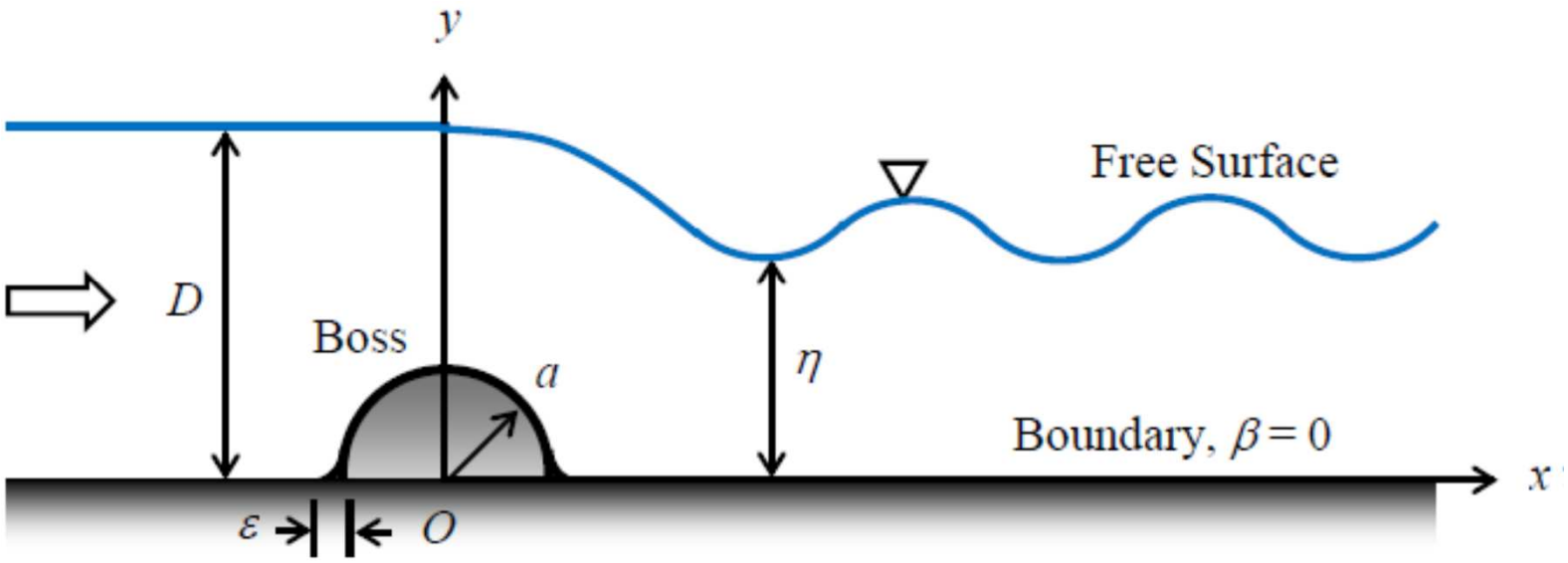


**Fig. 10** Schematic of flow over a hemi-cylindrical boss

$a$ = Radius of the submerged hemi-cylindrical boss

$D$ = Approach flow depth that is greater than the radius $a$ of boss

In order to have a gradual turn of the limiting streamlines at the base of the boss, it is assumed that the fillets of width $a\varepsilon$ on both sides of the base of the boss are attached

$\varepsilon$ = a factor

For this type of flow, Eq. (4) applies where $\beta = 0$ and $\tau_0 = \rho g n^2 U^2/(\eta - h)^{1/3}$

$$\frac{d^3\eta}{dx^3} + \frac{5}{2}\left[\frac{g(\eta-h)}{q^2} - \frac{1}{(\eta-h)^2}\right]\frac{d\eta}{dx} + \frac{7}{16}\cdot\frac{d^3h}{dx^3} + \frac{5}{2(\eta-h)^2}\cdot\frac{dh}{dx} + \frac{5}{2}\cdot\frac{gn^2}{(\eta-h)^{7/3}} = 0 \qquad (15)$$

By setting $\tilde{\eta} = (\hat{\eta} - 1)/\alpha$; $\alpha = a/D$; $\tilde{x} = x/a$; and $\tilde{h} = h/a$, Eq. (15) becomes

$$\frac{d^3\tilde{\eta}}{d\tilde{x}^3} + \frac{5\alpha^2}{2}\left\{\frac{1+\alpha(\tilde{\eta}-\tilde{h})}{F_0^2} - \frac{1}{[1+\alpha(\tilde{\eta}-\tilde{h})]^2}\right\}\frac{d\tilde{\eta}}{d\tilde{x}} + \frac{7}{16}\cdot\frac{d^3\tilde{h}}{d\tilde{x}^3} + \frac{5\alpha^2}{2}\cdot\frac{1}{[1+\alpha(\tilde{\eta}-\tilde{h})]^2}\frac{d\tilde{h}}{d\tilde{x}} + \frac{5\Omega\alpha^2}{2}\cdot\frac{1}{[1+\alpha(\tilde{\eta}-\tilde{h})]^{7/3}} = 0 \qquad (16)$$

where $\tilde{x}^2 + \tilde{h}^2 = 1$ on the surface of the boss, so that $d\tilde{h} / d\tilde{x} = -\tilde{x} / (1 - \tilde{x}^2)^{\frac{1}{2}}$ and $d^3\tilde{h} / d\tilde{x}^3 = -3\tilde{x}(1 - \tilde{x}^2)^{5/2}$

For $|\tilde{x}| \le 1 - \varepsilon$ (surface of the boss), writing $f = 1 + \left[ \tilde{\eta} - (1 - \tilde{x}^2)^{1/2} \right]$ yields

$$\frac{d^3\tilde{\eta}}{d\tilde{x}^3} + \frac{5\alpha^2}{2}\left( \frac{f}{F_0^2} - \frac{1}{f^2} \right)\frac{d\tilde{\eta}}{d\tilde{x}} - \frac{21}{26} \cdot \frac{\tilde{x}}{(1 - \tilde{x}^2)^{5/2}} - \frac{5\alpha^2}{2} \cdot \frac{\tilde{x}}{f^2 (1 - \tilde{x}^2)^{1/2}} + \frac{5\Omega\alpha^2}{2} \cdot \frac{1}{f^{7/3}} = 0 \qquad (17)$$

In the left fillet region, $\left|\tilde{x}+1\right| \le \varepsilon$, if $f_{-1} = 1+\alpha\left[\tilde{\eta} - m(\tilde{x}-1-\varepsilon)\right]$

where $m$ = slope given by $m = 0.5[(2-\varepsilon)\varepsilon]^{1/2}/\varepsilon$, then Eq. (17) becomes

$$\frac{d^3\tilde{\eta}}{d\tilde{x}^3} + \frac{5\alpha^2}{2}\left(\frac{f_{-1}}{F_0^2} - \frac{1}{f_{-1}^2}\right)\frac{d\tilde{\eta}}{d\tilde{x}} + \frac{5\alpha^2 m}{2}\cdot\frac{1}{f_{-1}^2} + \frac{5\Omega\alpha^2}{2}\cdot\frac{1}{f_{-1}^{7/3}} = 0 \qquad (18)$$

In the right fillet region, $\left|\tilde{x}-1\right| \le \varepsilon$, if $f_{+1} = 1+\alpha\left[\tilde{\eta} + m(\tilde{x}-1-\varepsilon)\right]$

Then, Eq. (17) becomes

$$\frac{d^3\tilde{\eta}}{d\tilde{x}^3} + \frac{5\alpha^2}{2}\left(\frac{f_{+1}}{F_0^2} - \frac{1}{f_{+1}^2}\right)\frac{d\tilde{\eta}}{d\tilde{x}} - \frac{5\alpha^2 m}{2}\cdot\frac{1}{f_{+1}^2} + \frac{5\Omega\alpha^2}{2}\cdot\frac{1}{f_{+1}^{7/3}} = 0 \qquad (19)$$

Beyond the fillet region $1+\varepsilon > \tilde{x} > -(1+\varepsilon),\ \hat{h} = 0$

Eq. (17) becomes

$$\frac{d^3\tilde{\eta}}{d\tilde{x}^3} + \frac{5\alpha^2}{2}\left(\frac{f}{F_0^2} - \frac{1}{f^2}\right)\frac{d\tilde{\eta}}{d\tilde{x}} + \frac{5\Omega\alpha^2}{2}\cdot\frac{1}{f^{7/3}} = 0\ , \quad f = 1+\alpha\tilde{\eta} \qquad (20)$$

Eqs. (17) – (20) are third-order ordinary differential equation and can be cast as systems of first order differential equations that can be integrated by Runge-Kutta method

For numerical computation, the approach flow Froude number is $F_0$ = 0.2 and the fillet dimension $\varepsilon$ = 0.1. The values of $\alpha$ are selected as 1/4 and 1/3

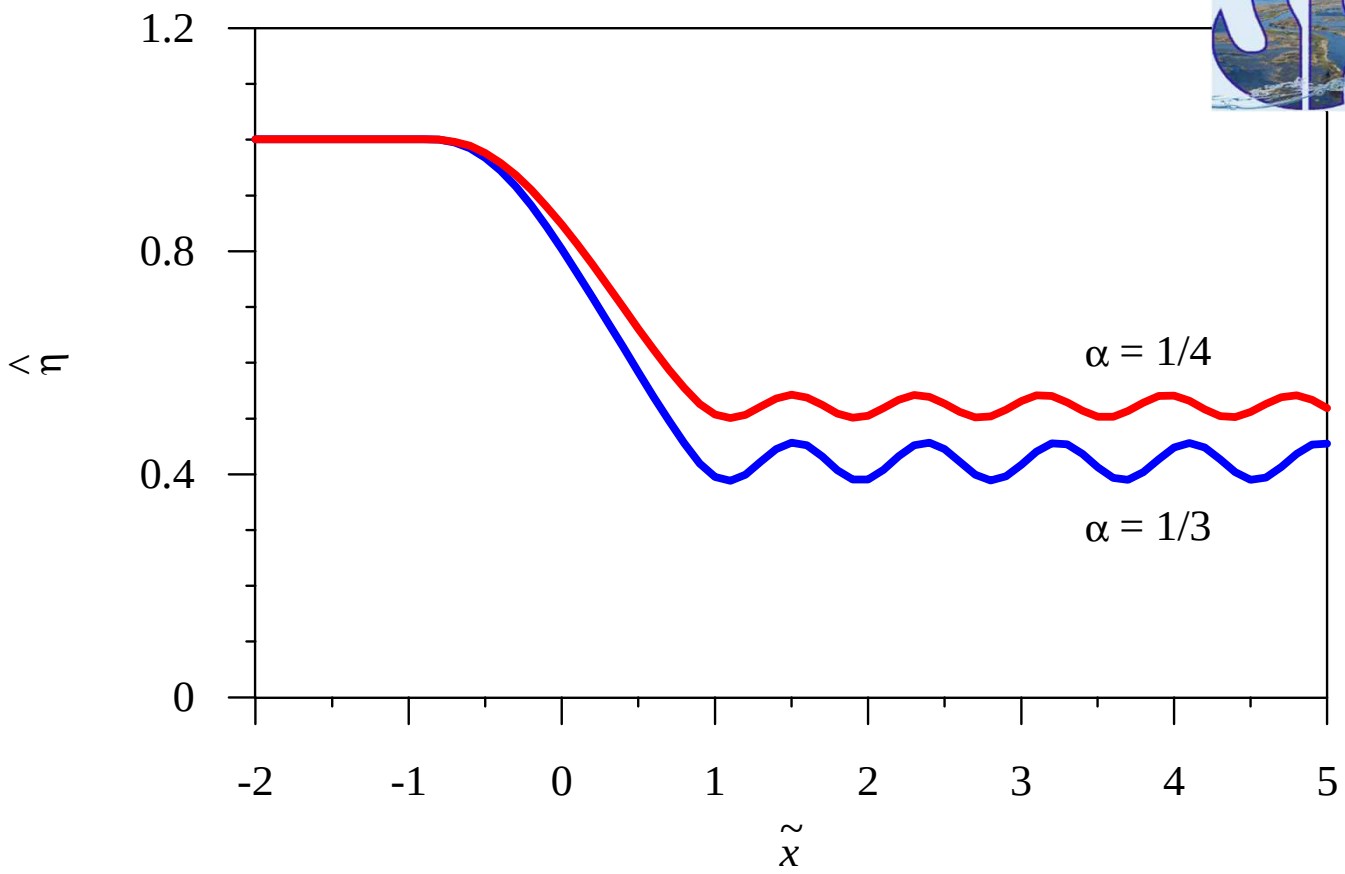


**Fig. 11** Normalized free surface profiles for flow over bosses having $\alpha$ = 1/4 and 1/3

There is a reduction in mean free surface elevation that exhibits undular profiles extending downstream

The amplitude of the waves diminishes with an increase in downstream distance $\tilde{x}$

The reduction in mean free surface elevation and the amplitude of the waves increase with an increase in $\alpha$

# Flow over a Sinusoidal Boundary

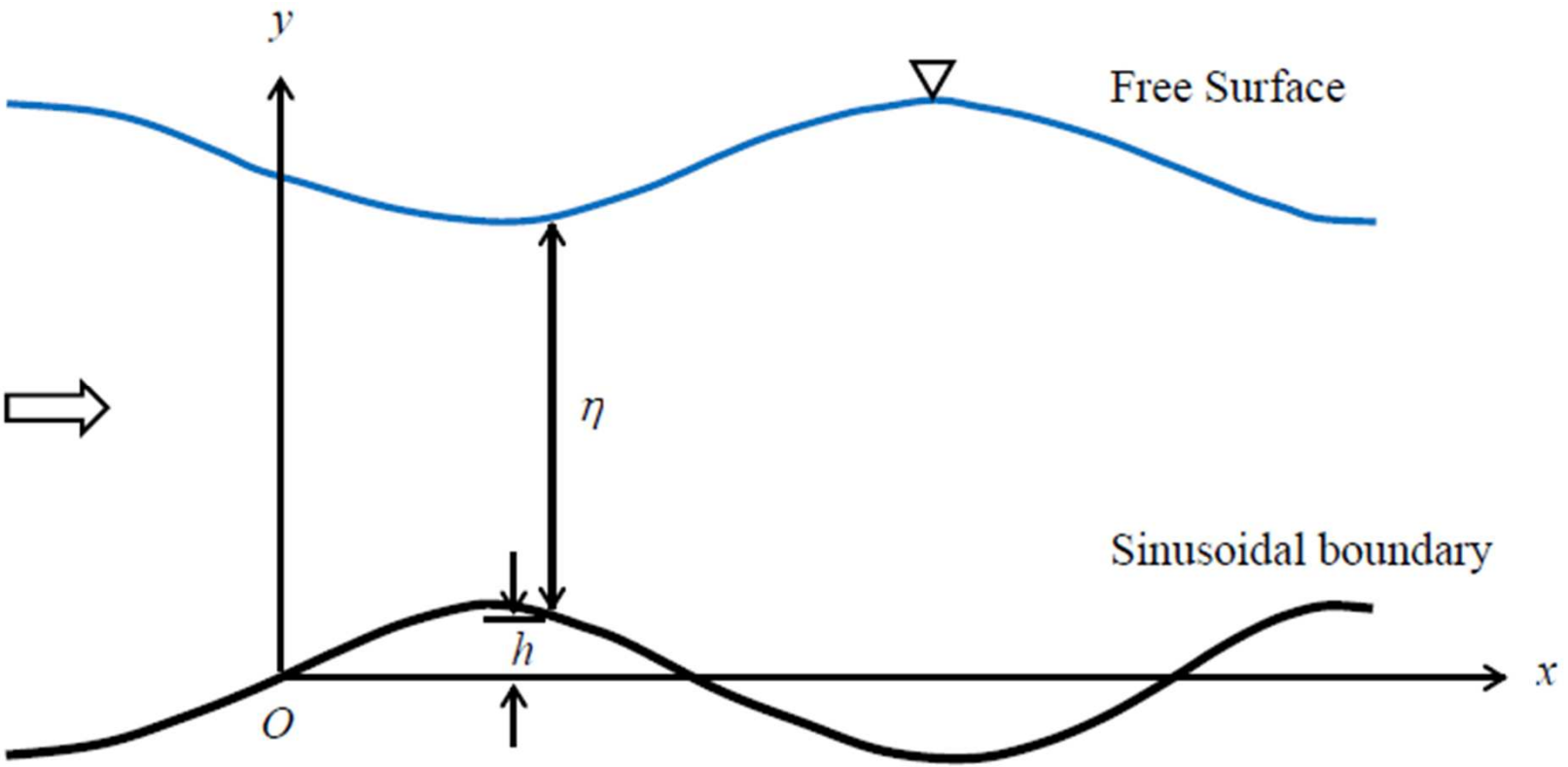


**Fig. 12** Schematic of flow over a sinusoidal boundary

- The $x$-axis is set through the mean boundary level, which is a horizontal line, and the origin $O$ is set conveniently on this axis

- The $y$-axis is therefore vertically upwards

- Due to the consideration of gradual variation of boundary undulation, the maximum boundary perturbation $|h|$ is small compared to the wave length and its streamwise gradient is $|\partial h/\partial x| << 1$

- The maximum free surface perturbation $|\eta|$ must be small and hence $|\partial \eta/\partial x| << 1$

The boundary has a sinusoidal form: $h = A \sin(kx)$; where $A$ = amplitude and $k$ = wave number. Introducing normalized quantities

$$\eta_0 = (\hat{\eta} - 1)/\delta;\ \delta = A/D;\ \xi = kx;\ \text{and}\ \sigma = kD$$

Eq. (4) for the free surface profile becomes

$$\frac{d^3\eta_0}{d\xi^3} + \frac{5}{2\sigma^2}\left(\frac{1}{f_s F_0^2} - \frac{1}{f_s^2}\right)\frac{d\eta_0}{d\xi} - \frac{7}{16}\cos\xi + \frac{5}{2\sigma^2}\cdot\frac{1}{f_s^2}\cos\xi + \frac{5\Omega}{2\delta\sigma^3}\cdot\frac{1}{f_s^{7/3}} = 0 \qquad (21)$$

where $f_s = 1 + \delta(\eta_0 - \sin\xi)$. The $\delta$ and $\sigma$ can be interpreted as normalized amplitude and wave number relative to mean flow depth $D$

- The solution of Eq. (21) must be periodic with a period $2\pi$
- A typical numerical experiment has been conducted for the values of $\delta$ = 0.1, $\sigma$ = 13, $F_0$ = 0.2 and $\Omega$ = 0.004
- Eq. (21) was then solved by Runge-Kutta method and periodicity of the solution was checked for five wavelengths of the boundary
- A satisfactory solution was obtained by taking the suitable initial values of $\eta_0$ = 0.8, $d\eta_0/d\xi$ = –0.71 and $d^2\eta_0/d\xi^2$ = –0.002 at the origin $\xi$ = 0 by trial
- The role of initial values is to initiate the computation for the periodical type of solution of differential equation [Fig. 13(a)]
- There is a spatial phase lag between the wavy free surface and the sinusoidal boundary. It is the normalized distance of a wave crest of free surface from that of the nearest boundary crest. The lag is 3

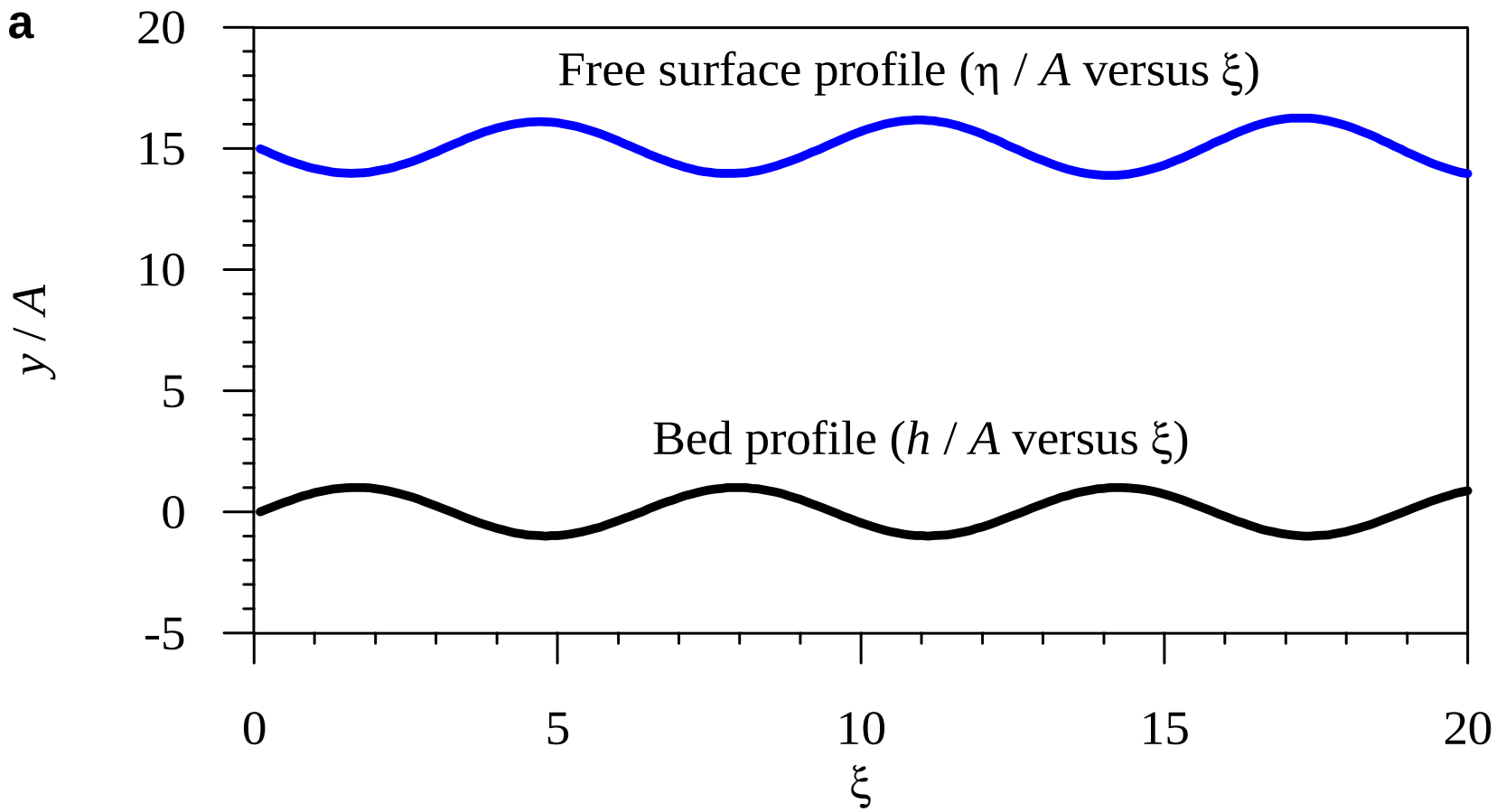


**Fig. 13** Normalized free surface profiles ($y/A$ versus $\xi$) for flow over sinusoidal boundaries: (**a**) For $\delta = 0.1$, $\sigma = 13$, $F_0 = 0.2$ and $\Omega = 0.004$

- In another numerical experiment, the value of $\sigma$ was reduced keeping the other parameters to remain unchanged
- The mean flow depth $D$ is reduced and made closer to the wavelength of the boundary profile
- Taking $\sigma = 9.5$, it was observed that the periodicity of $2\pi$ could not be attained
- The initial values that yielded closest to the periodicity were found to be $\eta_0 = 0.8$, $d\eta_0/d\xi = -1.41$ and $d^2\eta_0/d\xi^2 = -0.003$
- The profile of the free surface is plotted in Fig. 13(b), where the peaks of the waves definitely show periodic groups of waves in a heaving motion
- The effect becomes more pronounced for smaller values of $\sigma$

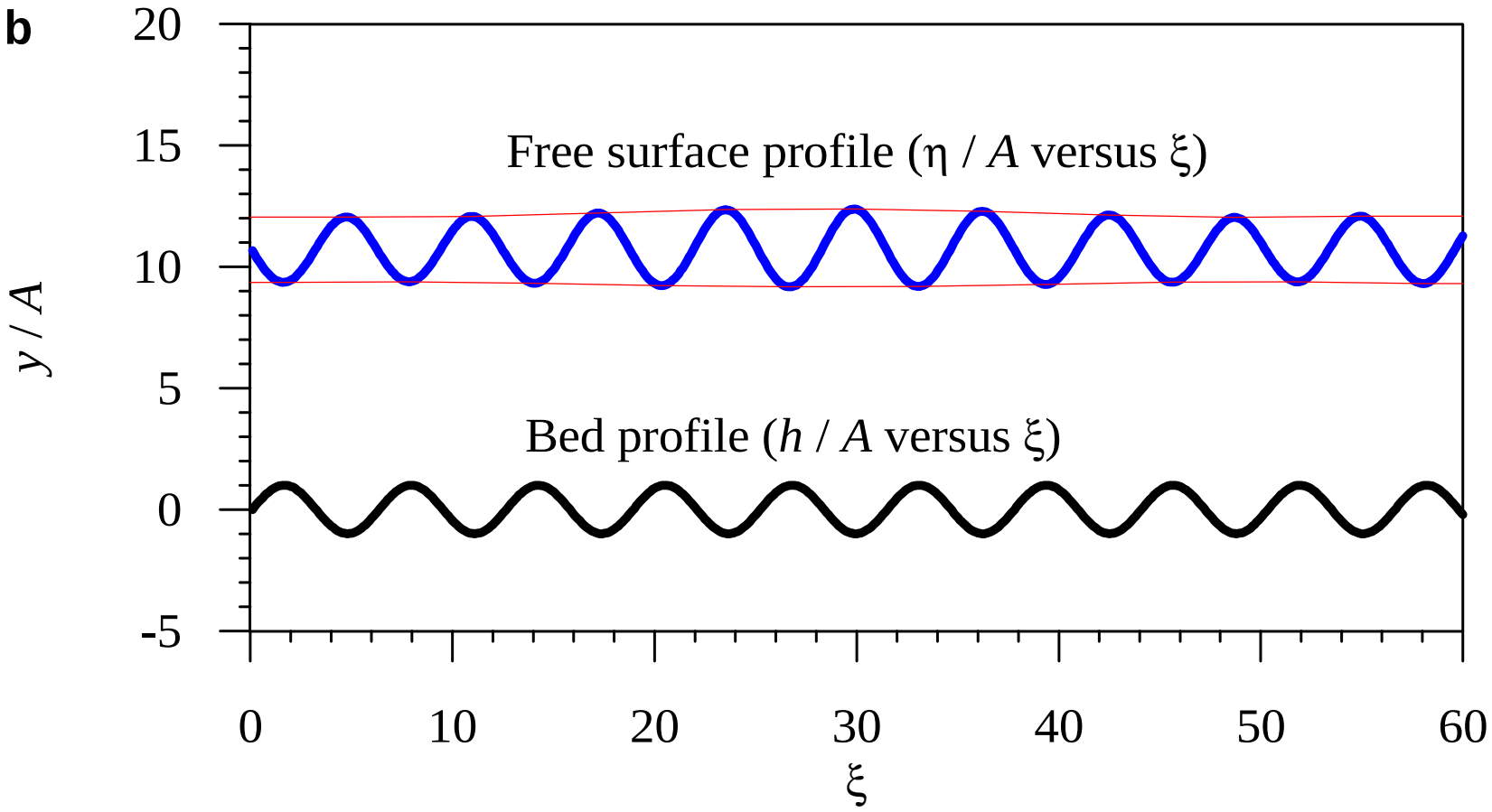


**Fig. 13** Normalized free surface profiles ($y/A$ versus $\xi$) for flow over sinusoidal boundaries: (**b**) For $\delta = 0.1$, $\sigma = 9.5$, $F_0 = 0.2$ and $\Omega = 0.004$

# Conclusions

- The undular hydraulic jump phenomenon can be treated by the instability principle of a third-order differential equation
- The threshold of an undular hydraulic jump is a monotonic increase of approach flow Froude number with boundary inclination
- The elevation of the undular free surface increases progressively as the boundary inclination increases
- The amplitude of the free surface waves decreases with an increase in downstream distance
- The elevation of first wave crest gets higher with an increase in approach flow Froude number
- The first wave height with respect to the conjugate flow depth increases with an increase in approach flow Froude number

- For the flow over a submerged hemi-cylindrical boss placed on the channel boundary, the steady-state flow analysis show that there is a drop in the free surface elevation on the downstream of the cylinder with an undular free surface profile

- For the shear flow over a sinusoidal boundary, the free surface elevation is adequately governed by a third-order ordinary differential equation
- The free surface profile lags the boundary profile
- When the flow depth decreases, an accumulation of heaved waves in the free surface is formed

# References

Akoz MS, Kirkgoz MS (2009) Numerical and experimental analyses of the flow around a horizontal wall-mounted circular cylinder. Transactions of the Canadian Society for Mechanical Engineers 33(2): 189-215

Akoz MS, Sahin B, Akilli H (2010) Flow characteristic of the horizontal cylinder placed on the plane boundary. Flow Measurement and Instrumentation 21: 476-487

Benjamin TB, Lighthill MJ (1954) On cnoidal waves and bores. Proceedings of the Royal Society of London A 224: 448-460

Bose SK, Dey S (2007) Curvilinear flow profiles based on Reynolds averaging. Journal of Hydraulic Engineering 133(9): 1074-1079

Bose SK, Dey S (2009) Reynolds averaged theory of turbulent shear flow over undulating beds and formation of sand waves. Physical Review E 80: 036304

Castro-Orgaz O (2010) Weakly undular hydraulic jump: Effects of friction. Journal of Hydraulic Research 48(4): 453-465

Chanson H (1993) Characteristics of undular hydraulic jumps. Research Report CE146, Department of Civil Engineering, University of Queensland, Brisbane, Australia

Chanson H (1995) Flow characteristics of undular hydraulic jumps: Comparison with near-critical flows. Research Report CH45/95, Department of Civil Engineering, University of Queensland, Brisbane, Australia

Chanson H (2000) Boundary shear stress measurements in undular flows: Application to standing wave bed forms. Water Resources Research 36(10): 3063-3076

Chanson H, Montes JS (1995) Characteristics of undular hydraulic jumps: Experimental apparatus and flow patterns. Journal of Hydraulic Engineering 121(2): 129-144

Dimaczek G, Tropea C, Wang AB (1989) Turbulent flow over two-dimensional, surface mounted obstacles: plane and axisymmetric geometries. Proceedings of the Second European Turbulence Conference, Berlin, Germany: 114-121

Durão DFG, Gouveia PST, Pereira JCF (1991) Velocity characteristics of the flow around a square cross section cylinder placed near a channel wall. Experiments in Fluids 11: 341-350

Fawer C (1937) Etude de quelques écoulements permanents à filets courbes. PhD thesis, Université de Lausanne, La Concorde, Lausanne, Switzerland (in French)

Good MC, Joubert PN (1968) The form drag of two-dimensional bluff plates immersed in the turbulent boundary layers. Journal of Fluid Mechanics 31: 547-582

Gotoh H, Yasuda Y, Ohtsu I (2005) Effect of channel slope on flow characteristics of undular hydraulic jumps. Transactions on Ecology and the Environment 83: 33-42

Grillhofer W, Schneider W (2003) The undular hydraulic jump in turbulent open channel flow at large Reynolds numbers. Physics of Fluids 15(3): 730-735

Hager WH, Hutter K (1984) On pseudo-uniform flow in open channel hydraulics. Acta Mechanica 53(3-4): 183-200

Henderson FM (1964) Steady flow in sinusoidally varying channels. Proceedings of the First Australasian Fluid Mechanics Conference: 51-67

Hsu ST, Kennedy JF (1971) Turbulent flow in wavy pipes. Journal of Fluid Mechanics 47: 481-502

Iwasa Y (1955) Undular jump and its limiting conditions for existence. Proceedings of the Fifth Japan National Congress for Applied Mechanics, Japan, II-14: 315-319

Iwasa Y, Kennedy JF (1968) Free surface shear flow over a wavy bed. Journal of Hydraulics Division 94(2): 431-454

Kaufmann K (1934) Hydromechanik II. Springer, Berlin

Mandrup-Andersen V (1978) Undular hydraulic jump. Journal of Hydraulics Division 104(8): 1185-1188

Mizumura K (1995) Free-surface profile of open-channel flow with wavy boundary. Journal of Hydraulic Engineering 121(7): 533-539

Montes JS (1998) Hydraulics of open channel flow. ASCE Press, Reston, VA, USA

Montes JS, Chanson H (1998) Characteristics of undular hydraulic jumps: Results and calculations. Journal of Hydraulic Engineering 124(2): 192-205

Motzfeld H (1937) Die turbulente stromung an welligen wanden. Zeitschrift für Angewandte Mathematik und Mechanik 17: 193-212

Nakayama A, Sakio K (2002) Simulation of flows over wavy rough boundaries. Annual Research Briefs, Center for Turbulence Research, Kobe University, Japan

Ohtsu I, Yasuda Y, Gotoh, H (2001) Hydraulic condition for undular jump formations. Journal of Hydraulic Research 39(2): 203-209

Ohtsu I, Yasuda Y, Gotoh H (2003) Flow conditions of undular hydraulic jumps in horizontal rectangular channels. Journal of Hydraulic Engineering 129(12): 948-955

Patel VC, Chon JT, Yoon JY (1991) Turbulent flow in a channel with a wavy wall. Journal of Fluid Mechanics 113(4): 579-586

Reinauer R, Hager WH (1995) Non-breaking undular hydraulic jump. Journal of Hydraulic Research 33(5): 1-16

Schulte H, Rouvé G (1986) Turbulent structures in separated flow. Proceedings of the Third International Symposium on Application of Laser Anemometry to Fluid Mechanics, Lisbon, Portugal: 2.2

Sforza PM, Mons RF (1970) Wall-wake: Flow behind a leading edge obstacle. AIAA Journal 8(2): 2162-2167

Tsai Y-P, Chou C-C (2008) Investigations of turbulent flow over solid wavy boundary. Chung Hua Journal of Science and Engineering 6(2): 9-14

Zhaoshun Z, Zhan C (1989) Numerical study of turbulent flows over wavy boundaries. Acta Mechanica Sinica 5(3): 197-204

**Thank you**